Eur. Phys. J. C (2010) 66: 187–196
DOI 10.1140/epjc/s10052-010-1239-0

THE EUROPEAN PHYSICAL JOURNAL C

Regular Article - Theoretical Physics

Confront *holographic* QCD with Regge trajectories of vectors and axial-vectors

Song He[1,a], **Mei Huang**[1,2], **Qi-Shu Yan**[3,4], **Yi Yang**[5,6]

[1]Institute of High Energy Physics, Chinese Academy of Sciences, Beijing, China
[2]Theoretical Physics Center for Science Facilities, Chinese Academy of Sciences, Beijing, China
[3]Department of Physics, University of Toronto, Toronto, Canada
[4]Department of Physics, National Tsing Hua University, Hsinchu, Taiwan
[5]Department of Electrophysics, National Chiao-Tung University, Hsinchu, Taiwan
[6]Physics Division, National Center for Theoretical Sciences, Hsinchu, Taiwan

Received: 7 May 2009 / Revised: 4 November 2009 / Published online: 15 January 2010

Abstract By matching the predictions of the Dp–Dq soft-wall model in type II superstring theory with the spectra of vector and axial-vector mesons, we show the dependence of the Regge trajectories parameters on the metric parameters of the model. From the experimental results of Regge parameters for vector mesons, it is found that the D3 background brane with both $q=5$ and $q=7$ probe brane and D4 background brane with $q=4$ probe brane are close to the realistic *holographic* QCD. We also discuss how to realize chiral symmetry breaking in the vacuum and asymptotic chiral symmetry restoration in high excitation states. We find that the constant component of the 5-dimension mass square of axial-vector mesons plays an efficient role to realize the chiral symmetry breaking, and a small negative z^4 correction in the 5-dimension mass square is helpful to realize the chiral symmetry restoration in high excitation states.

1 Introduction

Quantum Chromodynamics (QCD) has been accepted as the basic theory of describing the strong interaction for more than 30 years. However, it is still a challenge to solve QCD in the non-perturbative region where the gauge interaction is strong. In the early 1970's, string theory was proposed to describe strongly interacting particles [1–5]. Recently, the discovery of the gravity/gauge duality [6–8] has revived the hope to understand QCD in the strongly coupled region using string theory. The gravity/gauge, or anti-de Sitter/conformal field theory (AdS/CFT) correspondence provides a revolutionary method to tackle the problem of strongly coupled gauge theories. For a review of AdS/CFT, see [9].

The string description of realistic QCD has not been successfully formulated yet. Many efforts are invested in searching for such a realistic description by using the "top-down" approach, i.e. by deriving holographic QCD from string theory [10, 11], as well as by using the "bottom-up" approach, i.e. by examining possible *holographic* QCD models from experimental data [12–19].

In the "top-down" approach, many string induced models have been seriously studied recently by using string/gauge duality [6–8]. Different brane configurations, such as D3–D7, D4–D6 and D4–D8 etc. [20–23] were considered to describe QCD effectively. In these models, people extensively studied confinement, spontaneous chiral-breaking and thermal effects in QCD [24–27]. Meson, baryon and glueball spectra as well as their decay constants are also calculated [13, 28–31] and compared with experimental data. Till now, none of these models is completely successful. So far the best fitting one is the Sakai–Sugimoto (SS) model of D4–D8 branes' configuration, which can describe spontaneous chiral symmetry breaking naturally. However, there are many phenomena in QCD that still cannot be explained by the SS model; for example, the SS model fails to generate the linear Regge behavior.

It is an essential and crucial point for the realistic *holographic* QCD model to reproduce Regge behavior. Regge behavior is a well-known feature of QCD [32, 33], and it was the commanding evidence for suggesting the string-like structure of hadrons. A general empirical expression for Regge trajectories can be cast as

$$M_{n,S}^2 = a_n n + a_S S + b, \quad (1)$$

[a] e-mail: hesong@ihep.ac.cn

where n and S are the quantum number of high radial and spin excitations, respectively. The slope a_n and a_S have dimension GeV^2, and describe the mass square increase rate in radial excitations and spin excitations, respectively. In principle, a_n is not necessarily the same as a_S, though $a_n = a_S$ can be taken as a good approximation for fitting the experimental data [34]. The parameter b is the ground state mass square, and it is channel dependent.

On the other hand, many efforts have been made on the "bottom-up" approach. In this approach, one tries to extract the possible 5-dimension *holographic* QCD models from experimental data, and leaves the task of deriving the model from gravity to string theorists. The advantage of the "bottom-up" approach is that one can detect the possible 5-dimension space-time structure which is sensitive to the experimental observables. For example, in the "bottom-up" approach, it has been found that a z^2 dilaton field correction in the AdS_5 background leads to the linear behavior $M_n^2 \propto n$ [35]. The successful results in the "bottom-up" approach can provide a useful guide to the model building from the "top-down" approach. Considering the success of the SS model (one specific model based on D-brane backgrounds) in accommodating chiral symmetry breaking, instead of exploring the very generic background, we will concentrate on D-brane backgrounds in our "bottom-up" approach. To find the true D-brane configuration which can completely describe low energy QCD, there are many works to be done. In this work, we initialize a way to find a D-brane configuration which is able to explain as many as possible QCD phenomena by combining the "bottom-up" and "top-down" method. We hope that this way could be a guide to find the true D-brane scenario.

In this paper, by combing the "top-down" method and "bottom-up" method, i.e. by matching the Dp–Dq system in type II superstring theory with the Regge trajectories of meson spectra in the hidden local symmetry model with group $SU(2)_L \times SU(2)_R$, we investigate the possible background metric structure dual to realistic QCD. From the "top-down" approach, we systematically study the Dp–Dq system in this paper; by matching the linear Regge trajectories of vector and axial-vector meson spectra, we can know which Dp–Dq system is closer to the realistic *holographic* QCD model. From the "bottom-up" approach, we explore the realization of the chiral symmetry breaking in the vacuum and asymptotic chiral symmetry restoration in high excitation states. Our results can shed some light on the correct prescription of the string theory dual to the realistic QCD and is useful to construct a correct phenomenological *holographic* model.

The paper is organized as follows: After the introduction, we summarize the experimental data on Regge trajectories of vector and axial-vector mesons in Sect. 2. We derive the general 5-dimension metric structure of the Dp–Dq system in type II superstring theory in Sect. 3. In Sect. 4, we match the parameters of the 5-dimension metric with the parameters of the Regge trajectories. We then investigate the possible chiral symmetry breaking mechanisms to describe the splitting between the spectra of axial-vector mesons and that of the vector mesons in Sect. 5. We also discuss the possible way to restore chiral symmetry in high excitation states in Sect. 6. Finally, we present discussions and conclusions in Sect. 7.

2 Regge trajectories of vector and axial-vector mesons

In this paper, we carefully study realizing Regge trajectories of vector and axial-vector mesons in the *holographic* QCD model. We take the data of the radial and spin excitations of ρ and a from PDG2007 [36], which are listed in Table 1.

To describe Regge trajectories for both (ρ_1, ρ_3) and (a_1, a_3), we use the general formula (1). From the experimental data, the parameters of Regge trajectories can be determined by using the standard χ^2 fit. The parameters for (ρ_1, ρ_3) mesons and their correlations read

$$\begin{array}{l} a_n^\rho = +0.91 \pm 0.23 \\ a_S^\rho = +1.08 \pm 0.39 \\ b^\rho = -1.09 \pm 1.18 \end{array} \quad \begin{pmatrix} 1 & & \\ -0.82 & 1 & \\ +0.43 & -0.81 & 1 \end{pmatrix}. \tag{2}$$

The parameters for (a_1, a_3) mesons and their correlations read

$$\begin{array}{l} a_n^a = +0.81 \pm 0.22 \\ a_S^a = +0.88 \pm 0.39 \\ b^a = +0.13 \pm 1.17 \end{array} \quad \begin{pmatrix} 1 & & \\ -0.82 & 1 & \\ +0.43 & -0.81 & 1 \end{pmatrix}. \tag{3}$$

From the Regge trajectories of ρ and a, one can read off the information of chiral symmetry breaking in the vacuum and asymptotic chiral symmetry restoration in highly excited meson states.

Chiral symmetry breaking It is known that chiral symmetry is spontaneously broken in the vacuum, thus the observed chiral partners are not degenerate. From the Regge trajectories of the chiral partners ρ and a, the chiral symmetry breaking in the vacuum is reflected by the difference of the ground state square masses b^ρ and b^a. The difference is as large as $1\ \mathrm{GeV}^2$, i.e. $b^a - b^\rho \simeq M_{a_1}^2 - M_{\rho_1}^2 \simeq 1\ \mathrm{GeV}^2$.

Table 1 Vector and axial-vector meson spectra (in GeV)

n	1	2	3	4	5	6
$1^{--}_{\rho^n}$	0.770	1.450	1.700	1.900	2.150	2.270
$3^{--}_{\rho^n}$	1.690	1.990	2.250	–	–	–
$1^{++}_{a_1^n}$	1.260	1.640	1.930	2.095	2.270	2.340
$3^{++}_{a_3^n}$	1.870	2.070	2.310	–	–	–

Asymptotic chiral symmetry restoration in highly excited states It is noticed that the chiral partner becomes more and more degenerate in high excitations; see [37] and references therein. For example, for radial excitations of ρ_1 and a_1, the mass square difference of chiral partners $M_{a_1}^2 - M_{\rho_1}^2 = 0.9947\ \text{GeV}^2$ at $n = 1$, and this difference decreases to $0.3227\ \text{GeV}^2$ at $n = 6$; for the radial excitations of ρ_3 and a_3, the mass square difference of chiral partners $M_{a_3}^2 - M_{\rho_3}^2 = 0.6408\ \text{GeV}^2$ at $n = 1$, and it decreases to $0.2736\ \text{GeV}^2$ at $n = 3$. Recently Shifman et al. in [38] showed that it is difficult to realize chiral symmetry restoration in the *holographic* QCD model.

3 5-dimension metric structure of Dp–Dq soft-wall model

3.1 Metric structure of Dp–Dq system

In order to investigate the possible dual string theory for describing Regge behavior, we introduce the following Dp–Dq-branes system in type II superstring theory. In the Dp–Dq system, the N_c background Dp-brane describes the effects of pure QCD theory, while the N_f probe Dq-brane is to accommodate the fundamental flavors; this has been introduced by Karch and Katz [39]. Such a practice is well motivated from the string theory side. For example, in the Sakai–Sugimoto model, $p = 4$ and $q = 8$. The supergravity background is determined by solving the Einstein equation coupled with the N_c background Dp-branes; while low energy hadronic excitations, e.g. mesons, are described by open strings on the N_f probe branes, which are embedded in the supergravity background.

First, we consider N_c background Dp-branes in type II superstring theory. The near horizon solution in 10-dimension space-time is [40–42]

$$ds^2 = h^{-\frac{1}{2}} \eta_{\alpha\beta}\, dx^\alpha\, dx^\beta + h^{\frac{1}{2}} \left(du^2 + u^2\, d\Omega_{8-p}^2\right), \tag{4}$$

where $\alpha, \beta = 0, \ldots, p$, $\eta_{\alpha\beta} = \text{diag}(-1, 1, 1, \ldots)$. The warp factor $h(u) = (R/u)^{7-p}$ and R is a constant

$$R = \left[2^{5-p} \pi^{\frac{(5-p)}{2}} \Gamma\left(\frac{7-p}{2}\right) g_s N_c l_s^{7-p}\right]^{\frac{1}{7-p}}. \tag{5}$$

The dilaton field in this background has the form of

$$e^{\Phi} = g_s\, h(u)^{\frac{(p-3)}{4}}. \tag{6}$$

The effective coupling of the Yang–Mills theory is

$$g_{\text{eff}} \sim g_s N_c u^{p-3}, \tag{7}$$

which is u dependent. This u dependence corresponds to the RG flow in the Yang–Mills theory, i.e. the effective g_{eff} coupling constant depends on the energy scale u. In the case of the D3-brane, $g_{\text{eff}} \sim g_s N_c$ becomes a constant and the dual Yang–Mills theory is $\mathcal{N} = 4$ SYM theory, which is a conformal field theory. The curvature of the background (4) is

$$\mathcal{R} \sim \frac{1}{l_s^2 g_{\text{eff}}}, \tag{8}$$

which reflects the string/gauge duality—the string on a background of curvature $\mathcal{R}$ is dual to a gauge theory with the effective coupling g_{eff}. To make the perturbation valid on the string side, we require that the curvature is small, $\mathcal{R} \ll 1$, which means that the effective coupling in the dual gauge theory is large, $g_{\text{eff}} \gg 1/l_s^2$. In the case of the D3-brane, the curvature $\mathcal{R}$ becomes a constant, and the background (4) reduces to a constant curvature spacetime, $\text{AdS}_5 \times S^5$.

The coordinates transformation (for the cases of $p \neq 5$)

$$u = \left(\frac{5-p}{2}\right)^{\frac{2}{p-5}} R^{\frac{p-7}{p-5}} z^{\frac{2}{p-5}} \tag{9}$$

brings the above solution (4) to the following *Poincaré form*:

$$ds^2 = e^{2A(z)} \left[\eta_{\alpha\beta}\, dx^\alpha\, dx^\beta + dz^2 + \frac{(p-5)^2}{4} z^2\, d\Omega_{8-p}^2\right]. \tag{10}$$

Here we consider the background Dp-branes extended in $(p + 1)$ spacetime without compactification. Correspondingly, the dual QCD-like theory is in $(p + 1)$ dimensions, rather than in $(3 + 1)$ dimensions. Therefore, the glueball fields are defined to propagate in $(p + 1)$ dimensions. To study realistic QCD in $(3 + 1)$ dimensions, we must compactify the extra $(p - 3)$ dimensions of Dp-branes, similar to the procedure in the Sakai–Sugimoto model. After compactification of extra dimensions, the physical fields like glueball fields (with infinite Kaluza–Klein modes), are defined in $3 + 1$ dimensions. However, the ultraviolet (UV) properties of the glueball spectra are determined by the $A(z)$ term, which is only sensitive to the original background dimension p (and the dimensions q of the probe brane, which we will introduce shortly), but not to the detailed structure of the spacetime. To study these properties, we can use the results of the simplified model without considering the compactification.

Next, we consider the N_f probe Dq-branes with $q - 4$ of their dimensions in the S^{q-4} part of S^{8-p}, with the other dimensions in z and x^α directions as given in Table 2. The induced $q + 1$ dimensions metric on the probe branes is given as

$$ds^2 = e^{2A} \left[\eta_{\mu\nu}\, dx^\mu\, dx^\nu + dz^2 + \frac{z^2}{z_0^2}\, d\Omega_{q-4}^2\right]. \tag{11}$$

Table 2 Spacetime embedding of Dp–Dq system

	0	1	2	3	$\cdots$	p	z	S^{8-p}
Dp	•	•	•	•	•	•	–	–
Dq	•	•	•	•	–	–	•	$S^{q-4}\subset S^{8-p}$ –

Note here that we have introduced indices $\mu,\nu=0,\dots,3$ and $\eta_{\mu\nu}=\mathrm{diag}(-1,1,1,1)$ to indicate the $3+1$ dimensions which both Dp- and Dq-brane occupies. The metric (11) is conformal to $\mathrm{AdS}_5\times S^{q-4}$. The metric function of the warp factor only includes the logarithmic term

$$A(z)=-a_0\ln z,\quad \text{with } a_0=\frac{p-7}{2(p-5)},$$

and the dilaton field part takes the form of

$$e^{\Phi}=g_s\left(\frac{2}{5-p}\frac{R}{z}\right)^{\frac{(p-3)(p-7)}{2(p-5)}}. \tag{12}$$

It follows that

$$\Phi(z)\sim d_0\ln z,\quad \text{with } d_0=-\frac{(p-3)(p-7)}{2(p-5)}. \tag{13}$$

3.2 The deformed Dp–Dq soft-wall model

In the above subsection, we have derived the general metric structure of the Dp–Dq system in type II superstring theory, and we have noticed that the metric function $A(z)$ only includes the logarithmic term, and in general there is another logarithmic contribution to the dilaton field. However, from the lessons of the AdS_5 metric (D3 system) and the Sakai–Sugimoto model (D4–D8 system), the Dp–Dq system cannot describe linear trajectories of mesons. It was shown in [35], in order to produce linear trajectories, that there should be a z^2 term, but all z^2 asymptotics should be kept in the dilaton field $\Phi(z)$ and not in the warp factor $A(z)$. Otherwise, the radial slope a_n will be spin dependent. Therefore, to describe the real QCD, we propose a deformed Dp–Dq soft-wall model which is defined as

$$A(z)=-a_0\ln z,\qquad \Phi(z)=d_0\ln z+c_2z^2. \tag{14}$$

By assuming that the gauge fields are independent of the internal space S^{q-4}, after integrating out S^{q-4}, up to the quadratic terms and following the same assumption as in [35], we can have the effective 5D action for higher spin mesons described by tensor fields as

$$I=\frac{1}{2}\int d^5x\sqrt{g}e^{-\Phi(z)}\times\left\{\Delta_N\phi_{M_1\cdots M_S}\Delta^N\phi^{M_1\cdots M_S}+m_5^2\phi_{M_1\cdots M_S}\phi^{M_1\cdots M_S}\right\}, \tag{15}$$

where $\phi_{M_1\cdots M_S}$ is the tensor field and M_i is the tensor index. The value of S is equal to the spin of the field. The parameter m_5^2 is the 5D mass square of the bulk fields, and g and $\Phi(z)$ are the induced $q+1$-dimension metric and dilaton field as shown in (11) and (13). The action for the ρ_1,a_1 and ρ_3,a_3 mesons is given by taking $S=1$, and $S=3$, respectively.

Following the standard procedure of dimensional reduction, we can decompose the bulk field into its 4D components and their fifth profiles as

$$\phi(x;z)_{M_1\cdots M_S}=\sum_{n=0}\phi^n_{M_1\cdots M_S}(x)\psi_n(z).$$

The equation of motion (EOM) of the fifth profile wavefunctions $\psi_n(z)$ for the general higher spin field can be derived as

$$\partial_z^2\psi_n-\partial_zB\cdot\partial_z\psi_n+\left(M_{n,S}^2-m_5^2e^{2A}\right)\psi_n=0, \tag{16}$$

where $M_{n,S}$ is the mass of the 4-dimension field $\phi^n_{M_1\cdots M_S}(x)$ and

$$B=\Phi-k(2S-1)A=\Phi+c_0(2S-1)\ln z \tag{17}$$

is the linear combination of the metric background function and the dilaton field. The combination function $B(z)$ approaches the logarithmic asymptotic at UV brane, and goes to z^2 asymptotically at the infrared (IR) region. It is worthy of remark that the spin parameter S enters in the factor B and can affect the EOM and spectra. Two comments are in order.

(1) The EOM for the eigenspectrum and wavefunction is valid for all mesons with spin $S\geq 1$.
(2) The spin parameter S enters in the factor B and can affect the EOM and spectra.

The parameter k is a parameter depending on the induced metric (11) of the Dq-brane. After integrating out S^{q-4}, k is determined as

$$k=-\frac{(p-3)(q-5)+4}{p-7}. \tag{18}$$

It is obvious that k depends on both p and q. For simplicity, we have defined

$$c_0=ka_0=-\frac{(p-3)(q-5)+4}{2(p-5)}. \tag{19}$$

The parameters a_0,d_0, the other two parameters k,c_0 and the corresponding curvature $\mathcal{R}$ for any Dp–Dq system are listed in Table 3. We notice that $d_0=0$ for D3 background branes, i.e. the dilaton field is constant in AdS_5 space. However, the dilaton field in a general Dp–Dq system can have a $\ln z$ term contribution, e.g. in the D4–D8 system, $d_0=-3/2$. We also want to point out that for a pure

Table 3 Theoretical results for the Dp–Dq system

p	3		4			6	
q	5	7	4	6	8	4	6
$k=-\frac{(p-3)(q-5)+4}{p-7}$	1		1	5/3	7/3	1	7
$a_0=\frac{p-7}{2(p-5)}$	1		3/2			$-1/2$	
$c_0=ka_0$	1		3/2	5/2	7/2	$-1/2$	$-7/2$
$d_0=-\frac{(p-3)(p-7)}{2(p-5)}$	0		$-3/2$			3/2	
$\mathcal{R}\sim\frac{1}{g_{\text{eff}}}$	$1/\sqrt{3}$		$z^{-2}/\sqrt{36\pi}$			$6\sqrt{2}z^6$	

Dp–Dq system, the curvature is proportional to the inverse of the coupling strength g_{eff}. For D3 background branes, the curvature is a constant. The curvature for the D4 background branes is small at IR, and large at UV; its dual gauge theory is strongly coupled at IR and weakly coupled at UV, which is similar to QCD. However, the curvature for the D6 background branes is large at IR, and small at UV, its dual gauge theory is weakly coupled at IR and strongly coupled at UV, which is opposite to QCD.

It is noticed that even though there are top-down motivations from Dp–Dq system in type II superstring theory, the soft-wall Dp–Dq model that we propose in this subsection with a z^2 correction in the dilaton field is a model, not a solution to the supergravity equations of motion in type II string theory. However, in our proposed model, the values of $a_0, c_0, d_0, \mathcal{R}$ are determined by the Dp–Dq system and not related to the z^2 term in the dilaton field. Suppose the z^2 term correction in the dilaton field can be solved directly from the string theory, for example, by considering the backreaction from the probe flavor brane [17]; then one natural question is whether the $\ln z$ term in the dilaton profile will remain the same. From our experience in hadron physics, the $\ln z$ term dominates in the UV region ($z\to 0$), and can accommodate the Coulomb term in the effective potential, while the z^2 term dominates in the IR region ($z\to\infty$), which accommodates the linear term in the potential. Of course, there are also other terms, like z^4 or z^6, which should exist in the solution but physically their effects might be safely neglected. Such an understanding is also justified from the QCD sum rule approach. If the Dp–Dq system (with a suitable compactification) is indeed dual to the realistic QCD, then $\ln z$ and z^2 should be the most important terms which determine the spectra of the system. Therefore it is natural and intuitive to expect that the physics in the IR region will not affect the physics in the UV region. Actually, comparing to the $\ln z$ contribution, the deformation of the z^2 correction dominates the IR physics, but can be safely ignored in UV region.

4 Match soft-wall Dp–Dq system with Regge trajectories of vector and axial-vector mesons

In the dictionary of AdS/CFT, a f-form operator with conformal dimension Δ has 5-dimensional square mass $m_5^2=(\Delta-f)(\Delta+f-4)$ in the bulk [43], and for vector and axial-vector mesons $m_5^2=0$. The spectra of EOM of (16) for vector and axial-vector mesons has an exact solution:

$$M_{n,S}^2=4c_2n+4c_2c_0S+2c_2(1-c_0+d_0). \tag{20}$$

When $c_0=c_2=1$ and $d_0=0$, this solution reduces to the results given in the [35].

This exact solution supports the parameterization on Regge trajectories and can tell how the phenomenological parameters a_n, a_S and b are directly related with the metric parameters c_0, c_2 and d_0:

(1) c_2 is completely determined by the string tension in the radial direction a_n, i.e.

$$c_2=\frac{a_n}{4}. \tag{21}$$

Andreev in [44] shows that there is an upper bound of c_2. c_2 can be determined by the coefficient C_2 [45] of the quadratic correction to the vector–vector current correlator [46, 47]

$$\mathcal{N}q^2\frac{d\Pi_V}{dq^2}=C_0+\frac{1}{q^2}C_2+\sum_{n\geq 2}\frac{n}{q^{2n}}C_{2n}\langle\mathcal{O}_{2n}\rangle, \tag{22}$$

where C_2 can be determined from e^+e^- scattering data [48]. According to [44], the relation between C_2 in (22) and the parameter c_2 for the dilaton field is $c_2=-\frac{3}{2}C_2$. The experimental bound $|C_2|\leq 0.14\ \text{GeV}^2$ gives $|c_2|\leq 0.21\ \text{GeV}^2$. From the fitting result for the Regge trajectories of vector and axial-vector mesons (2) and (3), we can read that c_2 is around $0.2\sim 0.25$, which is in agreement with the experimental upper bounds.

(2) It is interesting to notice that c_0 reflects the difference of the string tension in the radial direction and spin direction,

$$c_0=\frac{a_S}{a_n}. \tag{23}$$

From the string theory side, it is commonly believed that the dual string theory of describing QCD should be strongly curved at high energy scales and weakly curved at low energy scales [10]. It seems that the D4 background brane system is more like the dual string theory of QCD. By reading the result for the Regge trajectories of vector and axial-vector mesons (2) and (3), we can see that a_S/a_n is around $1\sim 1.5$. By comparing with Table 3, we find that the D3 background brane with both $q=5$ and $q=7$ probe brane and the D4 background brane with $q=4$ probe brane are close to realistic QCD.

(3) Furthermore, d_0 can be solved for:

$$d_0 = \frac{2b}{a_n} + \frac{a_S}{a_n} - 1. \quad (24)$$

If we take the approximation of $a_n = a_S = 1$, we have $c_0 = 1$, $c_2 = 1/4$ for both vector and axial-vector mesons, while d_0 is mainly determined by the ground state square mass as $d_0^{\rho/a} = 2b^{\rho/a}$.

5 Dynamical chiral symmetry breaking

It is known that chiral symmetry is spontaneously broken in the vacuum; thus the observed chiral partners are not degenerate. From the Regge trajectories of the chiral partners ρ and a, the chiral symmetry breaking in the vacuum is reflected by the difference of the ground state square masses b^ρ and b^a. In order to describe the splitting between chiral partners ρ and a, we have to investigate the mechanism of dynamical chiral symmetry breaking.

5.1 Chiral symmetry breaking by the dilaton field

If we assume the 5D mass square $m_{5,\rho}^2 = m_{5,a}^2 = 0$, we can use (20) to fit the spectra of vector and axial-vector mesons. The central values and correlation matrix for vector mesons read

$$\begin{array}{l} c_0^\rho = +1.20^{+0.44}_{-0.40} \\ c_2^\rho = +0.23^{+0.06}_{-0.06} \\ d_0^\rho = -2.20^{+2.54}_{-1.70} \end{array} \quad \begin{pmatrix} 1 & & \\ -0.89 & 1 & \\ 0.83 & -0.99 & 1 \end{pmatrix}, \quad (25)$$

while the central values and correlation matrix for axial-vector mesons read

$$\begin{array}{l} c_0^a = +1.09^{+0.50}_{-0.44} \\ c_2^a = +0.20^{+0.06}_{-0.06} \\ d_0^a = +0.42^{+3.87}_{-2.34} \end{array} \quad \begin{pmatrix} 1 & & \\ -0.70 & 1 & \\ 0.62 & -0.99 & 1 \end{pmatrix}. \quad (26)$$

It is noticed that here c_2 and d_0 have dimension GeV^2. In our fitting, we have fixed $\Lambda_{\mathrm{Scl}} = 0.2$, $u_{\mathrm{UV}} = 0.1$ and $u_{\mathrm{IR}} = 3$, respectively. Boundary conditions for ρ mesons are given as

$$\psi_n^\rho|_{z=z_{\mathrm{UV}}} = 0, \qquad \partial_z \psi_n^\rho|_{z=z_{\mathrm{IR}}} = 0, \quad (27)$$

i.e. the Dirichlet type at UV and Neumann type at IR. Boundary conditions for axial-vector mesons a are given as Dirichlet type both at UV and IR, i.e.

$$\psi_n^a|_{z=z_{\mathrm{UV}}} = 0, \qquad \psi_n^a|_{z=z_{\mathrm{IR}}} = 0. \quad (28)$$

The 1σ contours of c_0 and c_2 are given in Fig. 1. There exists a large overlapping region in the parameter space of

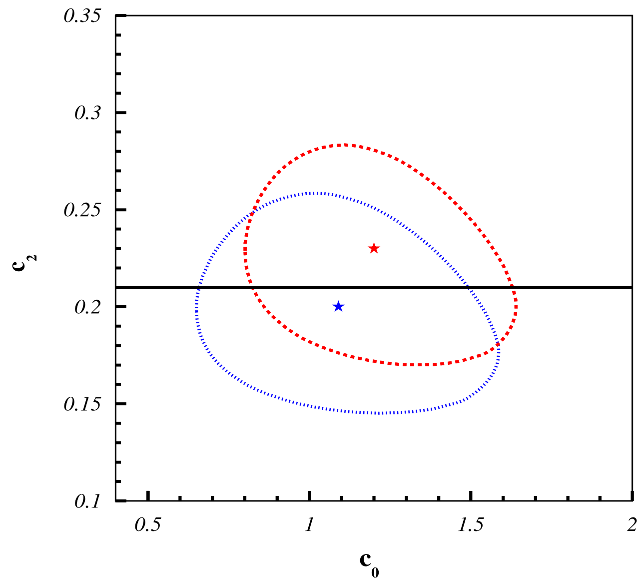

Fig. 1 The 1σ contours of c_0 and c_2 determined from the spectra of vector and axial-vector mesons with solutions given by (20), respectively. The *dashed* (*dotted*) *line* is determined by the vector (axial-vector) meson data. The best fit values are labeled as stars in the plot. The experimental upper bound (the *solid line*) of $c_2 = 0.21$ is drawn

c_0 and c_2, which means that it is possible to find a common region to accommodate the spectra data of both vector and axial-vector mesons. From Fig. 1 we can read that the allowed overlapping region is located with $0.17\ \mathrm{GeV} < c_2 < 0.21\ \mathrm{GeV}$ and $0.8 < c_0 < 1.6$.

The splitting of ρ and a can be described by different values of d_0, i.e. the chiral symmetry breaking can be described by the dilaton field. Unfortunately, from Table 3 we cannot find the corresponding Dp–Dq systems to describe vector and axial-vector mesons simultaneously. Therefore, we have to resort for other mechanisms to describe the chiral symmetry breaking.

Our fitting results show that c_0 prefers the value of $1 \sim 1.5$. From Table 3, we can read that for the D3–Dq background brane case, both $q = 5$ and $q = 7$ probe brane cases correspond to $c_0 = 1$, which is within the allowed overlapping region; for the D4 background brane case, only $q = 4$ case corresponds to $c_0 = 1.5$ which is within the allowed overlapping region; for D6 background brane case, no Dq probe brane case can be allowed in the allowed overlapping region. This indicates that the *holographic* QCD model should be close to models defined in Dp-brane background for $p = 3$ or 4. However, people usually take the approximation $a_n = a_s$, e.g. in [34]. In this case, $c_0 = 1$, the realistic *holographic* model is more like the soft-wall AdS_5 model.

We fix the following metric parameters to describe the spectra of vector mesons ρ:

$$c_0^{\rho} = 1,\quad c_2^{\rho} = 0.2\ \text{GeV}^2,\quad d_0^{\rho} = 0, \tag{29}$$

and these parameters are in the allowed region of (25). In the following, we discuss other possible ways of describing chiral symmetry breaking, i.e. we discuss how to realize axial-vector meson spectra in the soft-wall AdS$_5$ model defined in (29).

5.2 Chiral symmetry breaking by effective 5D mass square of axial-vector mesons in the Higgsless model

We determine the metric structure (29) of describing the vector mesons; now we need to describe the spectra of axial-vector mesons a in the same *holographic* QCD model. If we start from the Higgsless model (15), the only difference between the EOM for ρ and a is the 5D bulk mass m_5^2. $m_5^2 = 0$ for vector mesons, and we can expect that $m_5^2 \neq 0$ for axial-vector mesons due to chiral symmetry breaking.

For the general $A(z)$ and $\Phi(z)$ parameterized as

$$A(z) = -c_0 \ln z, \tag{30}$$

$$\Phi(z) = c_2 z^2, \tag{31}$$

the potential derived from $B(z) = \Phi(z) - (2S-1)A(z)$ can be put thus:

$$V(z) = 2c_2(m-1) + \frac{m^2 - \frac{1}{4}}{z^2} + c_2^2 z^2 + \frac{m_5^2}{z^{2c_0}}, \tag{32}$$

with

$$m = \frac{[(2S-1)c_0 + 1]}{2}. \tag{33}$$

When $c_0 = 1$, for any c_2 and constant m_5, the EOM

$$-\psi'' + V(z)\psi = M_n^2 \psi \tag{34}$$

can have an analytic solution:

$$M_n^2 = c_2(4n+1) + c_2(2S-1) + c_2\sqrt{\left[(2S-1)+1\right]^2 + 4m_5^2}. \tag{35}$$

When $S = 1$,

$$M_n^2 = 4c_2 n + 4c_2 + 2c_2\left(\sqrt{1+m_5^2} - 1\right). \tag{36}$$

From (36), for $m_{5,\rho}^2 = 0$ and $m_{5,a}^2 \neq 0$, we can get the spectra of the axial-vector a_1 through shifting the spectra of ρ_1 by $2c_2(\sqrt{1+m_{5,a}^2} - 1)$ upward. In Fig. 2, we explicitly show our numerical results of the spectra of axial-vector mesons a_1 by solving the EOM of a_1 (34) for different m_5^2. It is found that when $m_{5,a}^2 = 0.5\ \text{GeV}^2$, the produced a_1 spectra agree well with the experimental data. Note that here we have used the value of $m_{5,a}^2$ after scaling.

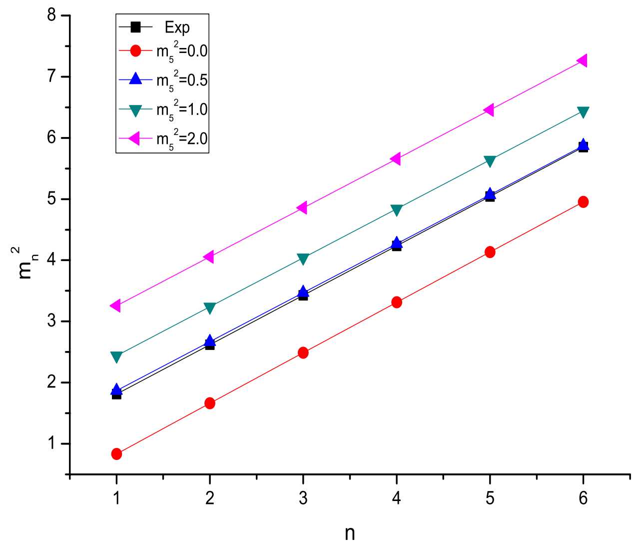

Fig. 2 The spectra of the axial-vector mesons a_1 by solving the EOM of a_1 (34) for different m_5^2

5.3 Chiral symmetry breaking by Higgs mechanism

In the Higgsless model, it is not clear how the axial-vector mesons gets an effective 5D mass. The Higgs mechanism in [35] offers such an explanation. It is suggested that the axial field picks up a z-dependent 5D mass via the Higgs mechanism from the background scalar X that encodes the chiral symmetry breaking. The axial-vector meson a_1 mode equation reads

$$\partial_z\left(e^{-\Phi(z)} e^{A(z)} \partial_z a_n\right) + \left[m_n^2 - g_5^2 e^{2A(z)} X(z)^2\right] e^{-\Phi(z)} e^{A(z)} a_n(z) = 0, \tag{37}$$

with $g_5^2 = 12\pi^2/N_c$. By comparing with the equation of motion of axial-vector mesons in the Higgsless model, we can regard $g_5^2 X(z)^2$ as the effective 5D mass square $m_{5,a}^2$ for axial-vector mesons, which is obtained by coupling with the scalar field. The linearized equation of motion for the scalar field X reads

$$\partial_z\left(e^{-\Phi(z)} e^{3A(z)} \partial_z X(z)\right) + 3e^{-\Phi(z)} e^{5A(z)} X(z) = 0. \tag{38}$$

It is quite complicated to solve the coupled (37) and (38). We only discuss two asymptotic solutions of scalar field at UV ($z = 0$) and IR, respectively.

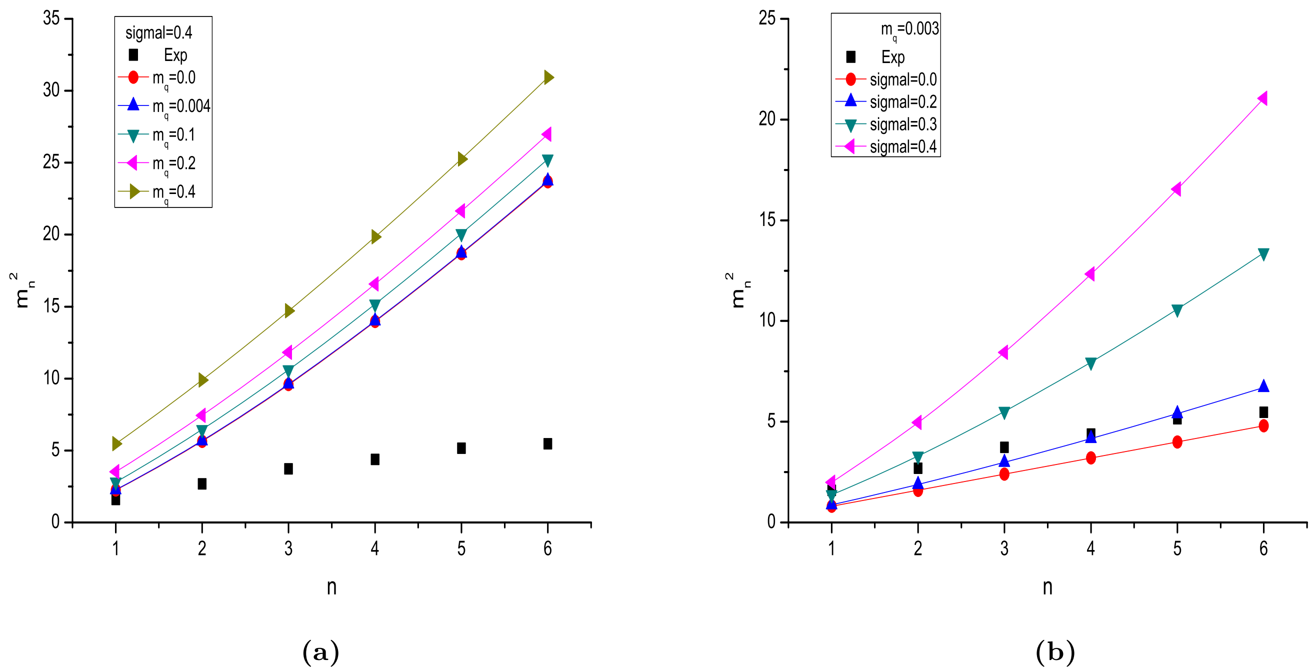

Fig. 3 The a_1 spectra by using the UV asymptotic form of the scalar field solution at $N_c = 3$, (**a**) is for different values of m_q with fixed $\Sigma = (400\text{ MeV})^3$, (**b**) is for different values of Σ with fixed $m_q = 3$ MeV

The asymptotic form at UV has the form of

$$X(z) \xrightarrow{z\to 0} \frac{1}{2} m_q z + \frac{1}{2}\Sigma z^3. \tag{39}$$

Here the coefficient m_q is the UV ($z = 0$) boundary condition given by the quark mass matrix, while the coefficient Σ is the chiral condensate, which can be determined dynamically by the boundary condition in the IR. We show the produced a_1 spectra from (39) in Fig. 3 when $N_c = 3$. Figure 3(a) is for different values of m_q with fixed $\Sigma = (400\text{ MeV})^3$, and Fig. 3(b) is for different values of Σ with fixed $m_q = 3$ MeV. It can be clearly seen that the asymptotic form at UV introduces non-linearity of the n dependence of M_n^2; the z^3 term contributes more on the non-linear behavior.

For large z (in the IR) on the background $\Phi = c_2 z^2$ the equation for X becomes

$$X'' - 2c_2 z X' + \frac{3}{z^2} X = 0 \quad (z \gg 1), \tag{40}$$

the scalar field has a solution that goes to a constant in the IR, i.e., $X(z) \to$ const as $z \to \infty$. $X(z) =$ const means the effective 5D mass $m_{5,a}^2 = g_5^2 X(z)^2$ is a constant. Then the spectra of a_1 will behave the same as that in Sect. 5.2.

6 Chiral symmetry restoration

Though the slopes in radial direction for vector mesons a_n^ρ and axial-vector mesons a_n^a can be roughly taken as the same, i.e, $a_n^\rho \simeq a_n^a$, in order to have chiral symmetry restoration in high excitation states, we need $a_n^\rho > a_n^a$.

Recently Shifman et al. in [38] showed that it is difficult to realize chiral symmetry restoration in the *holographic* QCD model. Here we propose a possibility to realize asymptotic chiral symmetry restoration in high excitation states. To accommodate such a case, we can take the ansatz that the effective 5D mass $m_5^2(z)$ has the following form:

$$\frac{m_5^2}{z^2} = \delta c_2^2 z^2 + \frac{\delta S^2}{z^2} + \delta m_0^2. \tag{41}$$

According to the experimental data given in (2–3), the numerical value of δc_2^2 should be around 20% of c_2^2. Substituting this ansatz into (32), we can find that the spectra can be exactly solved:

$$m_n^2 = 4c_2' n + 2c_2 S + 2c_2' S' + \delta m_0^2 + 2(c_2 + c_2'), \tag{42}$$

where

$$c_2' = \sqrt{c_2^2 + \delta c_2^2} \quad \text{and} \quad S' = \sqrt{S^2 + \delta S^2}.$$

Then equivalently, the chiral symmetry restoration demands that c_2' should be smaller than c_2, from which one infers that δc_2^2 should be negative. It is not clear at the moment how to get the negative correction $\delta c_2^2 z^4$ in 5D mass square of the axial-vector meson from the Higgs mechanism, which deserves further careful study in the future.

7 Conclusion and discussion

In summary, we have derived the general 5-dimension metric structure of the Dp–Dq system in type II superstring theory. We have shown the dependence of the Regge trajectories parameters on the metric parameters of the model.

(1) The quadratic term in the dilaton background field is solely determined by the slope in the radial direction.
(2) The warp factor is mainly determined by the difference of the slope in the spin direction and the radial direction.
(3) The logarithmic term in the dilaton background field contributes to the ground state square masses.

It is commonly believed that the dual string theory of describing QCD should be strongly curved at high energy scales and weakly curved at low energy scales, and it seems that the D4 background brane system is more like the dual string theory of QCD. However, the ratio of the slope in the spin direction of the vector mesons over its slope in the radial direction a_S/a_n is around 1–1.5, which indicates that the D3 background brane with both $q=5$ and $q=7$ probe brane, i.e., the AdS$_5$ soft-wall model and D4 background brane with $q=4$ probe brane are close to the *holographic* realistic QCD.

Considering $a_S/a_n=1$ is usually assumed to fit the Regge trajectories of mesons, and within this ansatz, we can conclude that the AdS$_5$ soft-wall model is a workable model. A constant 5D bulk mass for the axial-vector meson plays an efficient role to realize the chiral symmetry breaking in the vacuum, and a small negative z^4 correction in the 5D mass square is helpful to realize the chiral symmetry restoration in high excitation states.

The information in this study is important for a realistic *holographic* QCD model construction and our future study on the interactions of mesons, branching ratios and decay widths of mesons, etc. In our current approach, we chose the Higgsless model to describe the radial and higher spin excitations of vector and axial-vector mesons, the pseudoscalar π is the zero mode of axial-vector field and there are no radial and higher spin excitations. We leave the study of the Regge trajectories of scalar and pseudoscalar mesons by using the global symmetry breaking model to our future work.

Finally, we discuss the effect of a different boundary condition for axial-vector mesons on our final results. For realistic QCD chiral symmetry breaking, the boundary conditions should be consistent with the well-known QCD flavor structure: in the high energy or UV region, we expect that the chiral symmetry $SU_L(N_f)\times SU_R(N_f)$ is explicitly broken by quark masses; while in the low energy or IR region, we expect that the strong dynamics breaks the chiral symmetry further due to fermion condensates, but preserves the custodial isospin symmetry $SU_V(N_f)$. For such a symmetry breaking pattern, in the unitary gauge, it can be realized by choosing an axial-vector field with Dirichlet type conditions both at UV and IR; see, i.e. (28). Such boundary conditions have been adopted in (32–33) of [49] in the Higgsless model, for instance. In [14, 15], the boundary conditions for axial-vector mesons are given as the same as that for ρ mesons, i.e. with Dirichlet type at UV and Neumann type at IR,

$$\psi_n^a\big|_{z=z_{\mathrm{UV}}}=0,\qquad \partial_z\psi_n^a\big|_{z=z_{\mathrm{IR}}}=0. \tag{43}$$

We examine the effect of these two different boundary conditions on axial-vector meson spectra in Fig. 4, and find that these two different boundary conditions do not make too much difference for our final results.

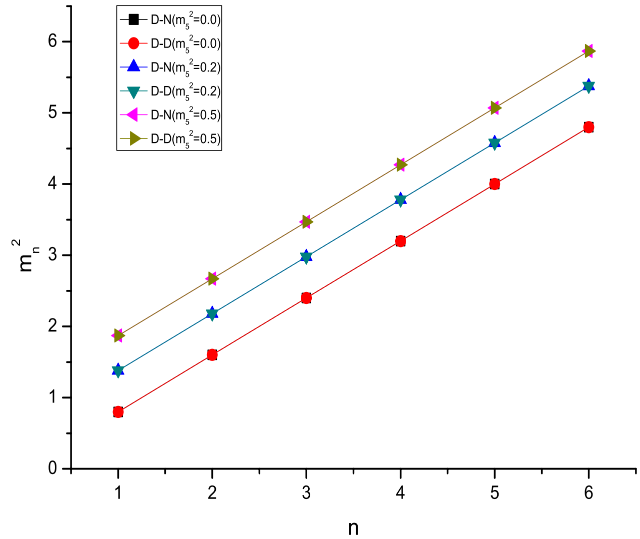

Fig. 4 The produced axial-vector meson spectra for different $m^2_{5,a}$ by using DD type boundary conditions (28) and DN type boundary conditions (43)

Acknowledgements We thank F.L. Lin, J. Liu, H.C. Ren and J. Shock for discussions. The work of M.H. is supported by the CAS program "Outstanding young scientists abroad brought-in", the CAS key project under grant No. KJCX3-SYW-N2, and NSFC under grant No. 10875134 and No. 10735040. The work of Q.Y. is supported by the NCS of Taiwan (No. NSC 95-2112-M-007-001 and 96-2628-M-007-002-MY3). The work of Y.Y. is supported by National Science Council (NCS) of Taiwan (97-2112-M-009-019-MY3) and National Center for Theoretical Sciences (NCTS) through NCS of Taiwan.

References

1. Y. Nambu, in *Symmetries and Quark Models*, ed. by R. Chand (Gordon and Breach, New York, 2001)
2. Y. Nambu, Phys. Rev. D **10**, 4262 (1974)
3. H.B. Nielsen, Submitted to the 15th *International Conference on High Energy Physics*, Kiev (1970)
4. H.B. Nielsen, P. Olesen, Nucl. Phys. B **61**, 45 (1973)
5. L. Susskind, Nuovo Cimento A **69**, 457 (1970)
6. J.M. Maldacena, Adv. Theor. Math. Phys. **2**, 231 (1998) [Int. J. Theor. Phys. **38**, 1113 (1999)]

7. S.S. Gubser, I.R. Klebanov, A.M. Polyakov, Phys. Lett. B **428**, 105 (1998)
8. E. Witten, Adv. Theor. Math. Phys. **2**, 253–291 (1998)
9. O. Aharony, S.S. Gubser, J. Maldacena, H. Ooguri, Y. Oz, Large N field theories, string theory and gravity. Phys. Rep. **323**, 183 (2000)
10. O. Aharony, arXiv:hep-th/0212193
11. A. Zaffaroni, PoS **RTN2005**, 005 (2005)
12. D.T. Son, M.A. Stephanov, Phys. Rev. D **69**, 065020 (2004)
13. G.F. de Teramond, S.J. Brodsky, Phys. Rev. Lett. **94**, 201601 (2005)
14. L. Da Rold, A. Pomarol, Nucl. Phys. B **721**, 79 (2005)
15. J. Erlich, E. Katz, D.T. Son, M.A. Stephanov, Phys. Rev. Lett. **95**, 261602 (2005)
16. K. Ghoroku, N. Maru, M. Tachibana, M. Yahiro, Phys. Lett. B **633**, 602 (2006). arXiv:hep-ph/0510334
17. J.P. Shock, F. Wu, Y.L. Wu, Z.F. Xie, J. High Energy Phys. **0703**, 064 (2007)
18. P. Colangelo, F. De Fazio, F. Jugeau, S. Nicotri, Phys. Lett. B **652**, 73 (2007)
19. J. Erdmenger, N. Evans, I. Kirsch, E. Threlfall, Eur. Phys. J. A **35**, 81 (2008). arXiv:0711.4467 [hep-th]
20. J. Babington, J. Erdmenger, N.J. Evans, Z. Guralnik, I. Kirsch, Phys. Rev. D **69**, 066007 (2004). arXiv:hep-th/0306018
21. M. Kruczenski, D. Mateos, R.C. Myers, D.J. Winters, J. High Energy Phys. **0405**, 041 (2004)
22. T. Sakai, S. Sugimoto, Prog. Theor. Phys. **113**, 843 (2005)
23. T. Sakai, S. Sugimoto, Prog. Theor. Phys. **114**, 1083 (2006)
24. D. Gepner, S. Sekahr Pal, Phys. Rev. D **76**, 125017 (2007)
25. N. Horigome, Y. Tanii, J. High Energy Phys. **0701**, 072 (2007)
26. K. Kajantie, T. Tahkokallio, J.-T. Yee, J. High Energy Phys. **0701**, 019 (2007)
27. D. Mateos, R.C. Myers, R.M. Thomson, J. High Energy Phys. **0705**, 067 (2007)
28. K. Hashimoto, T. Hirayama, A. Miwa, J. High Energy Phys. **0706**, 020 (2007)
29. D.K. Hong, T. Inami, H.-U. Yee, Phys. Lett. B **646**, 165–171 (2007)
30. K. Nawa, H. Suganuma, T. Kojo, Phys. Rev. D **75**, 086003 (2007)
31. D.K. Hong, M. Rho, H.-U. Yee, P. Yi, Phys. Rev. D **76**, 061901 (2007)
32. G. Veneziano, Nuovo Cimento A **57**, 190 (1968)
33. P.D.B. Collins, *An Introduction to Regge Theory and High Energy Physics* (Cambridge Univ. Press, Cambridge, 1975)
34. A.V. Anisovich, V.V. Anisovich, A.V. Sarantsev, Phys. Rev. D **62**, 051502 (2000)
35. A. Karch, E. Katz, D.T. Son, M.A. Stephanov, Phys. Rev. D **74**, 015005 (2006)
36. W.-M. Yao et al. (Particle Data Group), J. Phys. G **33**, 1 (2006) and 2007 partial update for the 2008 edition
37. L.Y. Glozman, arXiv:0710.0978 [hep-ph]
38. M. Shifman, A. Vainshtein, arXiv:0710.0863 [hep-ph]
39. A. Karch, E. Katz, J. High Energy Phys. **0206**, 043 (2002). arXiv:hep-th/0205236
40. G.W. Gibbons, K. Maeda, Nucl. Phys. B **298**, 741 (1988)
41. D. Garfinkle, G.T. Horowitz, A. Strominger, Phys. Rev. D **43**, 3140 (1991)
42. G.T. Horowitz, A. Strominger, Nucl. Phys. B **360**, 197 (1991)
43. E. Witten, Adv. Theor. Math. Phys. **2**, 253 (1998)
44. O. Andreev, Phys. Rev. D **73**, 107901 (2006)
45. L.S. Celenza, C.M. Shakin, Phys. Rev. D **34**, 1591 (1986)
46. M.A. Shifman, A.I. Vainstein, V.I. Zakharov, Nucl. Phys. B **147**, 385 (1979)
47. M.A. Shifman, A.I. Vainstein, V.I. Zakharov, Nucl. Phys. B **147**, 448 (1979)
48. S. Narison, Phys. Lett. B **300**, 293 (1993)
49. C. Csaki, J. Hubisz, P. Meade, arXiv:hep-ph/0510275